

Supplementary Information for

Graphene meta-interface for enhancing the stretchability of brittle oxide layers

Sejeong Won^{1,†}, Jae-Won Jang^{2,†}, Hyung-Jin Choi³, Chang-Hyun Kim¹, Sang Bong Lee¹, Yun Hwangbo¹, Kwang-Seop Kim¹, Soon-Gil Yoon³, Hak-Joo Lee¹, Jae-Hyun Kim^{1,*} and Soon-Bok Lee^{2,*}

¹Department of Nanomechanics, Nano-Convergence Mechanical Systems Research Division, Korea Institute of Machinery & Materials (KIMM), 156 Gajungbuk-ro, Yuseong-gu, Daejeon 305-343, Republic of Korea

² Department of Mechanical Engineering, Korea Advanced Institute of Science and Technology (KAIST), 291 Daehak-ro, Yuseong-gu, Daejeon 34141, Republic of Korea

³Department of Materials Science and Engineering, Chungnam National University, 99 Daehak-ro, Yuseong-gu, Daejeon 305-764, Republic of Korea

[†] These authors equally contributed to this work.

* Corresponding authors: jaehkim@kimm.re.kr, sblee@kaist.ac.kr

S1. Derivation of the shear-lag model

Strain transfer between the PET substrate and the ITO layer via the graphene layer can be described using the 2D shear lag model of McGuigan *et al.*³² The governing equation is derived from the force equilibrium relating the interfacial shear stress $\tau(x)$ of the graphene layer to the tensile stress σ transferred to the ITO layer; i.e.,

$$q \frac{d\sigma(x)}{dx} = -\tau(x) \quad (\text{S1})$$

The shear stress in the multilayer graphene is given by

$$\tau(x) = \frac{G(\varepsilon x - \Phi(x))}{p} \quad (\text{S2})$$

when $x \leq x_p$ and

$$\tau(x) = G\gamma_p = \tau_p \quad (\text{S3})$$

when $x \geq x_p$, where $\Phi(x)$ is the displacement of the ITO layer, ε is the applied strain and γ_p is the plastic shear strain in the multilayer graphene at which the shear stress reaches the critical value τ_p at $x = x_p$. Because the strain is the gradient of the displacement, we have

$$\sigma(x) = E \frac{d\Phi(x)}{dx}, \quad (\text{S4})$$

Combining Eqs. (S1) with (S2) yields the following differential equation:

$$\frac{d^2\Phi}{dx^2} - \beta^2\Phi(x) = -\beta^2\varepsilon x, \quad (\text{S5})$$

where $\beta = \sqrt{G/pqE}$. The following two boundary conditions are required to solve Eq. (S5):

$$\Phi(x=0) = 0 \quad (\text{S6})$$

and

$$\sigma(a) = E \frac{d\phi(x)}{dx} \Big|_{(x=a)} = 0. \quad (\text{S7})$$

The solution to Eq. (S5) is given by

$$\phi(x) = \varepsilon \left(x - \frac{\sinh(\beta x)}{\beta \cosh(\beta a)} \right). \quad (\text{S8})$$

The maximum stress occurs in the center of each segment, and we look for a solution where this stress is equal to the tensile strength σ^* , which corresponds to the maximum length of the segment before fracture at that strain. The tensile stress in the center of a segment is given by

$$\sigma(0) = \frac{1}{q} \int_0^a \tau(x) dx. \quad (\text{S9})$$

Substitution of Eqs. (S2) and (S3) into Eq. (S9) leads to the following expressions for the crack density n as a function of strain.

① The fully elastic case ($x_p > a$)

When maximum stress reaches the tensile strength, a is equal to half the maximum crack length; i.e.,

$$\sigma(0) = \frac{1}{q} \int_0^a \tau(x) dx = \sigma^* \quad (\text{S10})$$

and we have

$$a = \frac{1}{\beta} \cosh^{-1} \left(\frac{1}{1 - \frac{\sigma^*}{\varepsilon E}} \right) \quad (\text{S11})$$

Because the crack density is now given by $n = 1/2a$, we have

$$n = \frac{1}{2a} = \sqrt{\frac{G}{E}} \left[2\sqrt{pq} \cosh^{-1} \left(\frac{1}{1 - \frac{\sigma^*}{\varepsilon E}} \right) \right]^{-1} \quad (\text{S12})$$

② The elastic–plastic case ($x_p < a$)

When $x < x_p$, Eq. (S11) can be used for a ; i.e.,

$$\tau(x) = \frac{G}{p\beta} \left(\varepsilon - \frac{\sigma^*}{E} \right) \sinh(\beta x) \quad (\text{S13})$$

and when $x \geq x_p$ we have

$$\tau(x_p) = G\gamma_p. \quad (\text{S14})$$

Because we require that the shear stress is continuous at $x=x_p$, we obtain

$$x_p = \frac{1}{\beta} \sinh^{-1} \left(\frac{\gamma_p \sqrt{\frac{Gp}{qE}}}{\left(\varepsilon - \frac{\sigma^*}{E} \right)} \right), \quad (\text{S15})$$

and a is equal to half of the maximum crack length when the maximum stress becomes equal to the tensile strength. We therefore have

$$\sigma(0) = \frac{1}{q} \int_0^a \tau(x) dx = \frac{1}{q} \left(\int_0^{x_p} \tau(x) dx + \int_{x_p}^a G\gamma_p dx \right) = \sigma^* \quad (\text{S16})$$

which leads to

$$a = \frac{Eq}{G\gamma_p} \left[\left(\frac{\sigma^*}{E} - \varepsilon \right) \cosh \left(\sinh^{-1} \left(\frac{\gamma_p \sqrt{\frac{Gp}{Eq}}}{\left(\varepsilon - \frac{\sigma^*}{E} \right)} \right) \right) + \varepsilon + \gamma_p \sqrt{\frac{GP}{Eq}} \sinh^{-1} \left(\frac{\gamma_p \sqrt{\frac{Gp}{Eq}}}{\left(\varepsilon - \frac{\sigma^*}{E} \right)} \right) \right]. \quad (\text{S17})$$

Because the crack density is $n = 1/2a$, this can be expressed as follows:

$$n = \frac{G\gamma_p}{2Eq} \left[\left(\frac{\sigma^*}{E} - \varepsilon \right) \cosh \left(\sinh^{-1} \left(\frac{\gamma_p \sqrt{\frac{Gp}{Eq}}}{\left(\varepsilon - \frac{\sigma^*}{E} \right)} \right) \right) + \varepsilon + \gamma_p \sqrt{\frac{GP}{Eq}} \sinh^{-1} \left(\frac{\gamma_p \sqrt{\frac{Gp}{Eq}}}{\left(\varepsilon - \frac{\sigma^*}{E} \right)} \right) \right]^{-1}. \quad (\text{S18})$$

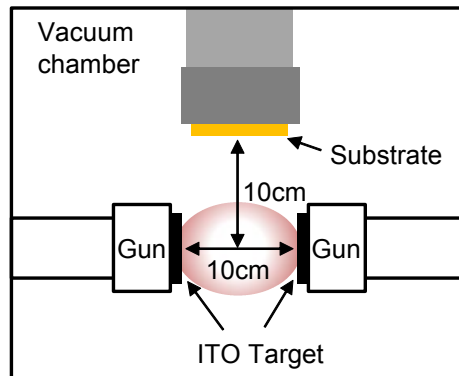


Figure S1. Schematic of an off-axis RF magnetron sputtering.

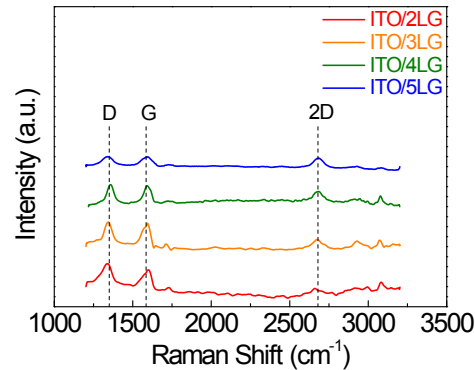


Figure S2. Raman spectra (excitation wavelength $\lambda = 514\text{nm}$) of the ITO/MLG after subtracting the peaks of PET substrates. The existence of the D peak indicates the damage on the graphene layers during ITO sputtering, but even with this damage, the graphene meta-interface can reduce the strain transfer by the interlayer sliding. By decreasing the sputtering damage of graphene, the performance of the graphene meta-interface can be improved further.

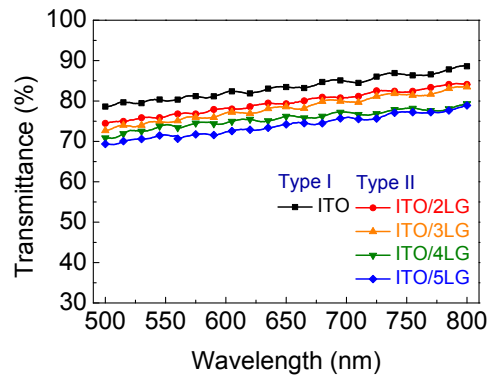


Figure S3. Transmittances of type-I and type-II structures over a range of wavelength.

Samples		Transmittance (%)	
		Mean	Standard deviation
Type-I	ITO	80.7	0.86
Type-II	ITO/2L G	76.6	0.57
	ITO/3L G	74.5	0.18
	ITO/4L G	74.1	0.64
	ITO/5L G	72.1	0.69

Table S1. Transmittances of type-I and type-II structures at a wavelength of 550 nm.

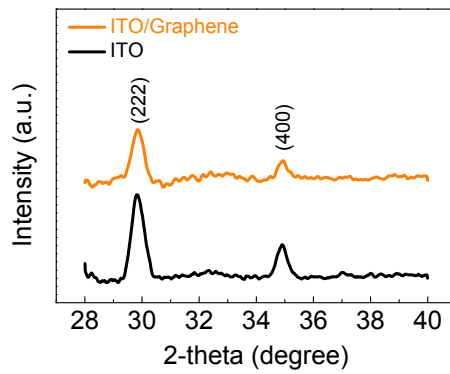


Figure S4. XRD diffraction patterns of ITO and ITO/graphene on the PET substrates.

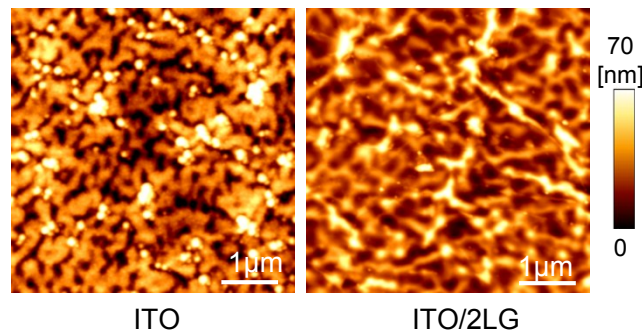


Figure S5. Topographies of ITO and ITO/2LG on PET substrates.

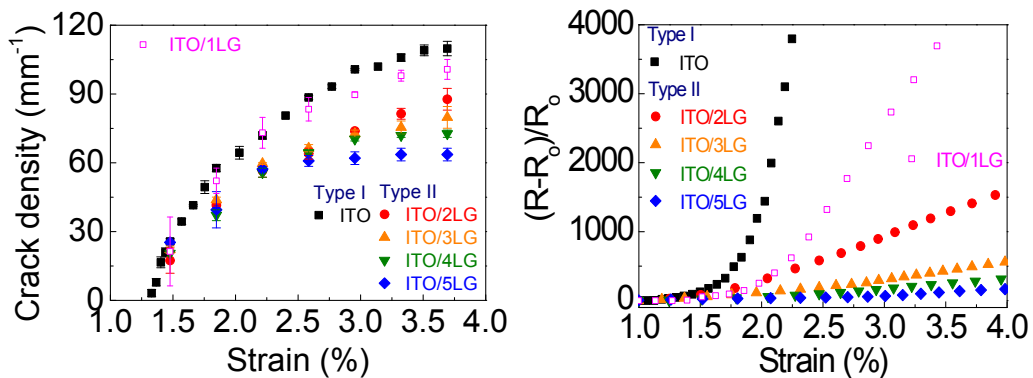


Figure S6. Crack densities and the normalized electrical resistance for the ITO/1LG. a) Crack densities for the ITO/1LG, type-I and type-II structures as a function of the strain. b) The normalized electrical resistance of the ITO/1LG, type-I and type-II structures as a function of the strain.